Accessibility of selenomethionine proteins by total chemical synthesis: structural studies of human herpesvirus-8 MIP-II

Weiping Shao[a], Elias Fernandez[b], Jill Wilken[c], Darren A. Thompson[c], Michael A. Siani[c], John West[a], Elias Lolis[b,*], Barry I. Schweitzer[a]

[a] *Walt Disney Memorial Cancer Institute at Florida Hospital, 12722 Research Parkway, Orlando, FL 32826, USA*
[b] *Department of Pharmacology, Yale University School of Medicine, 333 Cedar Street, New Haven, CT 06510, USA*
[c] *Gryphon Sciences, 250 East Grand Avenue, Suite 90, San Francisco, CA 94080, USA*

Received 8 October 1998

Abstract The determination of high resolution three-dimensional structures by X-ray crystallography or nuclear magnetic resonance (NMR) is a time-consuming process. Here we describe an approach to circumvent the cloning and expression of a recombinant protein as well as screening for heavy atom derivatives. The selenomethionine-modified chemokine macrophage inflammatory protein-II (MIP-II) from human herpesvirus-8 has been produced by total chemical synthesis, crystallized, and characterized by NMR. The protein has a secondary structure typical of other chemokines and forms a monomer in solution. These results indicate that total chemical synthesis can be used to accelerate the determination of three-dimensional structures of new proteins identified in genome programs.

Key words: X-ray crystallography; Nuclear magnetic resonance; vMIP-II; Kaposi sarcoma; Herpesvirus-8; Genome

1. Introduction

Genome sequencing programs are identifying proteins at a pace that far exceeds the rate at which these proteins can be characterized. The problem is particularly acute for high resolution structural studies, which normally require cloning, overexpression, and purification to produce milligram quantities of proteins. Moreover, for X-ray crystallography, crystallization and phase determination can be very time-consuming. The replacement of methionine for selenomethionine allows multiwavelength anomalous diffraction (MAD) to be used for solving the phase problem and can accelerate the determination of three-dimensional structures [1]. The incorporation of selenomethionine into proteins typically requires growth of cells in the presence of selenomethionine under conditions where the methionine biosynthetic pathway is blocked. This requirement once again necessitates the cloning, overexpression, and purification of the selenomethionine-modified proteins.

Total chemical synthesis is an alternative means for producing proteins for structural studies [2]. Production of pure protein by this method can occur rapidly following identification of a new protein sequence. This method of production has been successfully applied to an increasing number of nuclear magnetic resonance (NMR) studies. The determination of X-ray structures has been limited to a smaller number of proteins owing to the strict requirements for homogeneous samples required for crystallization. Recent advances in chemical synthesis have now made possible the desired quality of sample for X-ray structural studies. Proteins or domains of up to 150 amino acids with appropriately spaced cysteine residues are accessible by total chemical synthesis using thioester-mediated native chemical ligation [2].

The chemokine superfamily is comprised of proteins ranging in size between 7 and 15 kDa [3]. These proteins are generally involved in recruiting cells of the immune system to sites of infection or tissue injury. A number of chemokine homologues and their receptors are encoded by viral genomes. The human herpesvirus 8 (HHV-8) is the infectious agent responsible for Kaposi sarcoma in patients with and without HIV infection [4]. The HHV-8 genome encodes two genes with sequence similarity to the human CC chemokine family. HHV-8 macrophage inflammatory proteins (MIP)-I (vMIP-I) and MIP-II (vMIP-II) exhibit 37.9 and 41.1% amino acid identity to MIP-1α, respectively [5]. The amino acid identity between vMIP-I and vMIP-II is 48%, thus they are more closely related to each other than to cellular chemokines, suggesting that they have evolved by gene duplication within the virus genome rather than by independent acquisition from the host genome. Both vMIP-I and vMIP-II partially inhibit HIV-1 infection of peripheral blood mononuclear cells. vMIP-II was shown to block infection of HIV-1 on a CD4 positive cell line expressing CCR3 and to a lesser extent on one expressing CCR5 [6]. vMIP-II has also been shown to inhibit entry of HIV into T cells, mediated through CXCR4 [7]. Consequently, this protein may serve as a lead for development of broad-spectrum anti-HIV chemokine receptor antagonists.

In the present study, we demonstrate the accessibility of selenomethionine ([SeMet])-vMIP-II to total chemical synthesis and establish the utility of chemically synthesized selenomethionine-proteins for structural studies. The secondary structure of [SeMet]-vMIP-II has been determined by two-dimensional homonuclear and heteronuclear NMR spectroscopy. Furthermore, [SeMet]-vMIP-II has been crystallized and the selenium sites determined by Patterson methods.

*Corresponding author. Fax: (1) (203) 785-7670.
E-mail: elias.lolis@yale.edu

Abbreviations: DQF-COSY, double quantum filtered correlation spectroscopy; HSQC, heteronuclear single quantum coherence; IL-8, interleukin-8; MCP, monocyte chemoattractant protein; MIP, macrophage inflammatory protein; NMR, nuclear magnetic resonance; NOE, nuclear Overhauser effect; RANTES, regulated upon activation, normal T-cell expressed and presumably secreted; RMS, root mean square; ROESY, rotating frame Overhauser effect spectroscopy; [SeMet]-vMIP-II, selenomethionine-vMIP-II; TOCSY, total correlation spectroscopy

PII: S0014-5793(98)01520-8

2. Materials and methods

2.1. Total chemical synthesis of vMIP-II and [SeMet]-vMIP-II

vMIP-II was prepared by thioester-mediated native chemical ligation of unprotected peptide segments [2]. The peptide segments were synthesized by solid-phase methods either manually or on an Applied Biosystems 430A Peptide Synthesizer. The ligation product, the polypeptide vMIP-II[(1–74)(-SH)$_4$] was purified and folded in 2 M guanidine HCl, 100 mM Tris, pH 8, containing 8 mM cysteine and 1 mM cystine. The amino acid sequence corresponds to residues 21–94 for vMIP-II (GenBank accession number U75698). In the selenomethionine-modified protein, Met-66 was replaced with a selenomethionine residue to facilitate X-ray crystallographic studies. *N*-α-Fmoc-seleno-L-methionine was prepared from commercially available seleno-L-methionine (Sigma) and incorporated quantitatively into the peptide chain preactivated as the 1-hydroxy-7-azobenzotriazole ester. The resulting native and selenomethionine proteins were purified by reversed-phase HPLC and characterized by electrospray ionization mass spectrometry (Fig. 1). The observed mass for the native and [SeMet]-vMIP-II was 8400.4 and 8445.8 Da, respectively. These compare favorably with the calculated mass (average isotope composition) of 8397.9 and 8444.8 Da for 2 disulfides in native and [SeMet]-vMIP-II, respectively.

2.2. Crystallography

Lyophilized protein was dissolved in water at a concentration of 10 mg/ml. The vapor diffusion method was used to identify crystallization conditions. Crystals were first observed from 20% polyethylene glycol 4000, 20% isopropanol, and 0.1 M citrate, pH 5.6. Crystals grow in 2–3 days from optimized conditions. Crystals were equilibrated in cryoprotectant consisting of mother liquor with 15% glycerol. Diffraction data to 2.8 Å were collected from crystals frozen in a stream of N_2 at −160°C and measured with a RAXIS-IIC image plate detector (Rigaku, Tokyo) using a Rigaku RU200 rotating anode X-ray generator (operating at 50 mA and 100 kV) equipped with a Yale double mirror system. X-ray data were processed with DENZO and SCALEPACK [8]. The merging *R*-factors were 0.072 and 0.076 for the native and [SeMet]-vMIP-II, respectively.

2.3. NMR spectroscopy

NMR samples were prepared by dissolving the lyophilized protein in 90% H_2O/10% D_2O or D_2O containing 50 mM phosphate and 0.1 mM NaN_3. The pH was adjusted to pH 3.25 by adding microliter increments of DCl or NaOD to a 0.6-ml sample. The final protein concentration of [SeMet]-vMIP-II used for the detailed NMR analysis was 2 mM. Preparation of the MIP-2 sample has been previously described [29].

All NMR experiments were carried out on a Varian UNITY Plus 600-MHz spectrometer. The majority of NMR spectra were recorded at a temperature of 308 K; some experiments were also recorded at 303 K and 313 K to resolve ambiguities. Clean total correlation spectroscopy (TOCSY) [9–11] experiments were carried out with mixing times of 14, 30, 65, 80 and 100 ms. Nuclear Overhauser effect spectroscopy (NOESY) [12,13] experiments were carried out with mixing times of 50, 100, 150 and 200 ms. A rotating frame Overhauser effect spectroscopy (ROESY) [14] experiment was carried out with a mixing time of 35 ms. A double quantum filtered correlation spectroscopy (DQF-COSY) experiment [15] was also performed. All spectra were recorded in the phase-sensitive mode according to the method of States et al. [16], with spectral widths of 8.5 kHz in both dimensions. The water resonance in TOCSY and NOESY spectra was suppressed by using the WET solvent suppression technique [17]. Twenty ms selective pulses with a SEDUCE [18] profile were employed in these experiments. In other experiments, low power pre-irradiation of the water resonance was used for solvent suppression.

The spectra were processed and analyzed using Felix 95 (Molecular Simulations, San Diego, CA, USA). Prior to Fourier transformation in t_2, the NOESY and TOCSY data were multiplied by a weak Lorentzian to Gaussian window function and zero-filled to yield final spectra of 2 K×2 K points. DQF-COSY data were processed using an exponential weighting in t_2 and a sine-bell function in t_1 and zero-filled to 8 K×1 K points. Additional suppression of the water signal was achieved by convolution of the time-domain data.

A 2D ^{1}H-^{15}N heteronuclear single quantum coherence (HSQC) experiment [19] was acquired at natural abundance. GARP-1 was used to decouple ^{15}N during the acquisition period. The ^{1}H and ^{15}N carriers were placed at the water frequency and 119.0 ppm, respectively, with spectral width of 8.5 kHz (^{1}H) and 6 kHz (^{15}N). The acquired data consisted of 64 complex data points in t_1 (^{15}N) and 2048 complex data points in t_2 (^{1}H). Zero-filling and linear prediction were employed to yield a final spectrum of 2048 (^{15}N)×2048 (^{1}H) points.

Slow amide proton exchange with solvent was measured at 308 K by repeated acquisition of TOCSY spectra, acquired 0.5 h following dissolution of the lyophilized protein sample in D_2O. The total acquisition time for a TOCSY spectrum was approximately 2 h. Qualitative hydrogen exchange rates were derived by comparison of amide proton cross-peak volumes as a function of acquisition time.

The quaternary structure (i.e. monomer vs. dimer) of vMIP-II was investigated by employing pulsed field gradient NMR self-diffusion measurements as described by Altieri et al. [20]. The water-suppressed LED pulse sequence was used for these measurements. The value of the coefficient of self-diffusion, D_s, was obtained by fitting the signal attenuation as a function of gradient strength to Eq. 1:

$$A(2\lambda) = A(0)\exp[-(\gamma\delta G)2(\Delta-\delta/3)D_s] \quad (1)$$

where $\gamma = {}^1$H gyromagnetic ratio, δ=PFG duration (s), G = gradient strength (G/cm), and Δ = time between PFG pulses (s). Gradients were calibrated using a spin-echo experiment.

3. Results and discussion

3.1. Crystallization

Crystals of vMIP-II have symmetry of space group P1 with cell constants of $a = 47.00$ Å, $b = 45.64$ Å, $c = 45.48$ Å, $\alpha = 101.43$, $\beta = 115.04$, and $\gamma = 110.86$. The presence of a metal ion such as Ni^{2+} results in a space group with C2 symmetry and dimensions $a = 71.58$ Å, $b = 58.62$ Å, $c = 49.73$ Å, $\beta = 131.85$, with two molecules in the asymmetric unit. Attempts to solve the structure of either crystal form by molecular replacement using various modifications of MIP-1β, regulated upon activation, normal T-cell expressed and presumably secreted (RANTES), and monocyte chemoattractant protein (MCP)-1 as probes were unsuccessful. It is therefore likely that vMIP-II displays significant structural differences from other β-chemokines. Data collected from both native and [SeMet]-vMIP-II have been used to calculate a difference Patterson map (Fig. 2). The positions of the two selenium sites (one per monomer in the asymmetric unit) were solved and refined with the PHASES suite of programs (W. Furey, University of Pittsburgh). The structure will now be solved by multiwavelength anomalous diffraction using the [SeMet]-MIP-II crystals from data collected at a synchrotron radiation source.

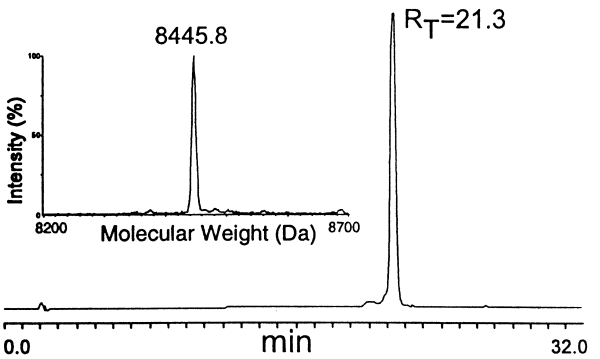

Fig. 1. Characterization of purified [SeMet]vMIP-II. Main panel: Analytical reversed-phase HPLC. Conditions: 5–65% acetonitrile and 0.1% TFA in water over 30 min. Inset: Hypermass reconstruction of the ESI-MS spectrum observed mass 8445.8 Da; calculated mass (average isotope composition) 8444.8 Da.

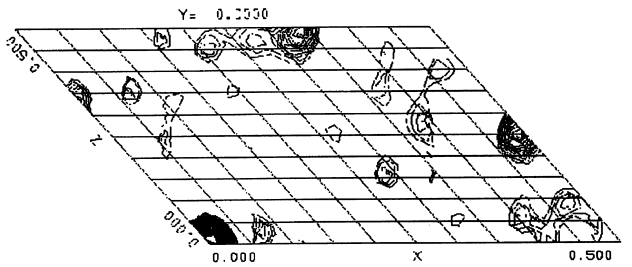

Fig. 2. Difference Patterson map for the [SeMet]-vMIP-II. The positions of the two selenium sites in the Patterson map are $u=0.32$, $v=0.0$, $w=0.48$ and $u=0.49$, $v=0.0$, $w=0.24$, and refine to $x=0.17$, $y=0.10$, $z=0.24$ and $x=0.24$, $y=0.00$, $z=0.13$ as determined by the PHASES package.

3.2. NMR assignments

The sequential assignment of the residues in the ^{1}H-NMR spectrum was achieved by first identifying spin systems using TOCSY spectra acquired with different mixing times and DQF-COSY spectra. This procedure was followed by assigning identified spin systems to particular residues in the protein by the observation of sequential HN-HN, C$^\alpha$H-HN, and C$^\beta$H-HN NOEs [30]. Ambiguities arising from degenerate chemical shifts were resolved by recording spectra at different temperatures ranging from 303 to 313 K. The side-chain NH resonances were not fully resolved in the ^{1}H spectra but could be resolved in a 2D ^{15}N-^{1}H HSQC spectrum (Fig. 3) and linked with C$^\beta$H or C$^\gamma$H resonances by NOEs in the NOESY spectra. ^{15}N and ^{1}H chemical shifts are listed in Table 1.

3.3. Secondary structure

The secondary structure of vMIP-II was determined from a qualitative analysis of the sequential, medium-range and some long-range backbone NOE intensities, backbone scalar coupling constants, amide proton exchange rate and chemical shift analysis of C$^\alpha$H protons. vMIP-II contains a three-stranded anti-parallel β-sheet, characterized by stretches of strong sequential ($d_{\alpha N}(i,i+1)$) NOE connectivities, long-range backbone NOE connectivities ($d_{NN}(i,j)$, $d_{\alpha N}(i,j)$ and $d_{\alpha\alpha}(i,j)$) (Fig. 4), reduced amide proton exchange rates and the C$^\alpha$H

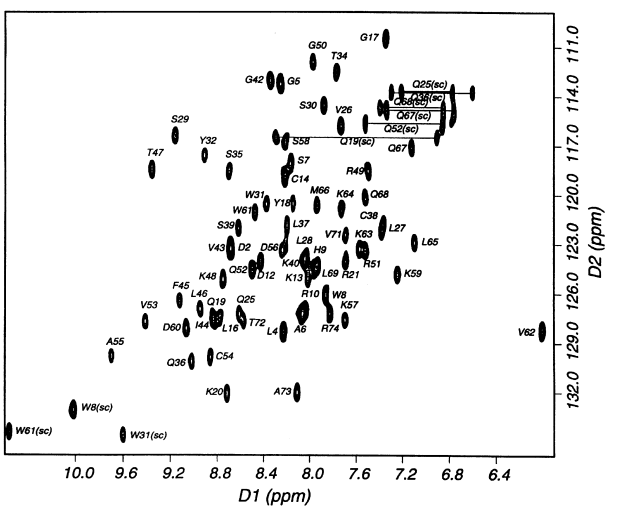

Fig. 3. ^{1}H-^{15}N-HSQC spectrum recorded at 600 MHz. The assignments obtained in this study are indicated. The side-chain amide resonances of individual Gln residues are connected by horizontal lines.

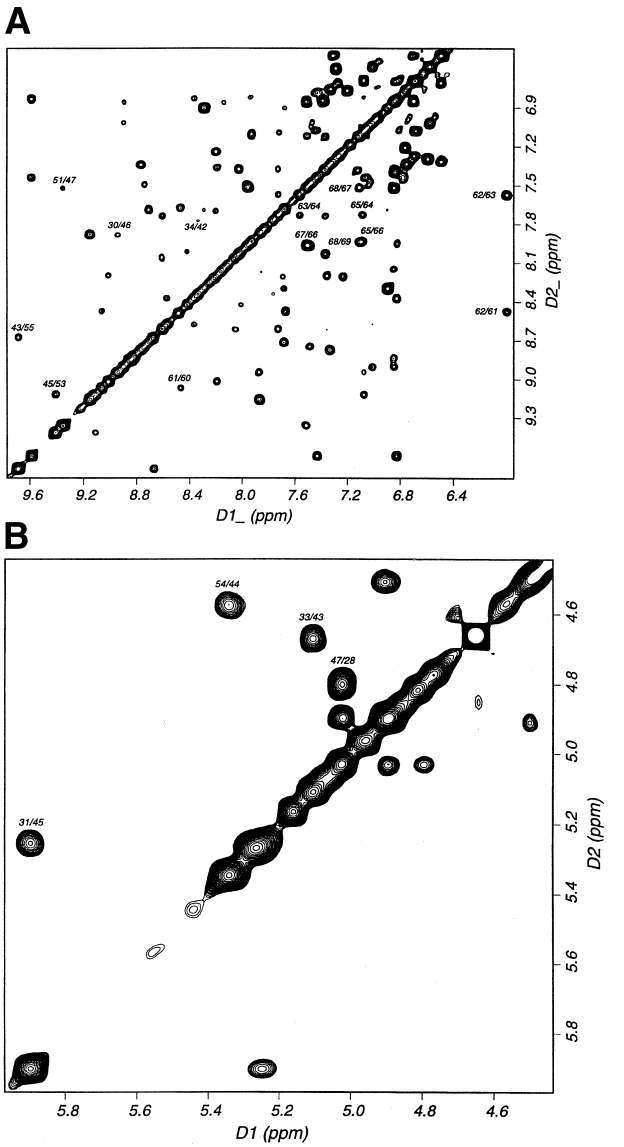

Fig. 4. Regions of the NOESY (150 ms) spectrum of vMIP-II recorded at 600 MHz. The assignments obtained in this study are indicated. A: Amide-amide region. B: Hα-Hα region.

chemical shift index of Wishart et al. [21] (Fig. 5). The arrangement of the three β-strands into an anti-parallel β-sheet is that of a Greek key: strand 2 (residues 43–46) is hydrogen bonded to strands 1 (residues 30–33) and 3 (residues 52–55). In addition, a C-terminal α-helix extending from 60 to 68 is well-defined, as characterized by the observed grouping of $d_{NN}(i,i+1)$, $d_{NN}(i,i+2)$, $d_{\alpha N}(i,i+3)$, and $d_{\alpha\beta}(i,i+3)$ NOE connectivities. Determination of the tertiary structure from NOE distance constraints is now underway.

3.4. Quaternary structure

Dimerization is a characteristic feature of most chemokines [22]. For most members of the CXC chemokine family (MIP-2, MGSA, interleukin-8 (IL-8), NAP-2 and PF-4), the two monomers associate to form an extended six-stranded β-sheet with most of the subunit-subunit interactions formed between the first β-strand of each monomer. (The tetramers of NAP-2 and PF-4 are formed by back-to-back association of the extended β-sheets of the two dimers.) The dimer interface of the

Table 1
Chemical shifts of vMIP-II in H_2O solution at 308 K and pH 3.12

Residue	^{15}N	H^N	H^α	H^β	Others
Gly1		8.35	3.76, 4.13		
Asp2	126.95	8.68	4.83	2.80, 2.87	
Thr3		8.21	4.30	4.20	$C^\gamma H_3$ 1.17
Leu4	128.40	8.22	4.31	1.55, 1.64	H^γ –; $C^\delta H_3$ 0.80, 0.84
Gly5	113.31	8.25	3.90, 3.90		
Ala6	127.39	8.06	4.28	1.30	
Ser7	118.08	8.17	4.36	3.80, 3.80	
Trp8	125.99	7.86	4.56	3.17, 3.17	$H^{\delta1}$ 7.17; $H^{\varepsilon1}$ 10.01; $H^{\zeta2}$ 7.38; $H^{\eta2}$ 7.14; $H^{\varepsilon3}$ 7.51; $H^{\zeta3}$ 7.06; $N^{\varepsilon1}$ 133.12
His9	124.30	7.92	4.47	2.89, 3.05	$H^{\delta2}$ 7.06; $H^{\varepsilon1}$ 8.54
Arg10	126.95	8.04	4.23	1.70, 1.58	H^γ 1.41, 1.53; H^δ 3.07; H^ε 7.13
Pro11			4.41	2.20	H^γ 1.92, 1.96; H^δ 3.56, 3.69
Asp12	124.11	8.42	4.68	2.75, 2.80	
Lys13	125.22	8.02	4.46	1.80, 1.91	H^γ 1.44; H^δ 1.71; H^ε 2.97
Cys14	118.95	8.20	5.05	3.46, 2.66	
Cys15		8.85	4.68	2.64, 2.64	
Leu16	127.53	8.76	4.27	1.58	H^γ 1.58; $C^\delta H_3$ 0.83, 0.90
Gly17	110.51	7.34	3.70, 3.70		
Tyr18	120.59	8.13	4.85	3.13, 2.70	H^δ 6.85; H^ε 6.69
Gln19	127.38	8.84	4.33	2.07, 2.46	H^γ 2.63; $N^\varepsilon H$ 6.89, 8.29; N^ε 116.59
Lys20	132.11	8.71	4.48	1.94, 1.94	H^γ 1.52, 1.64; H^δ 1.78; H^ε 3.09
Arg21	124.11	7.69	4.42	1.56	H^γ 1.56; H^δ 3.12; $N^\varepsilon H$ 7.13
Pro22			1.84	1.06, 1.10	H^γ 0.59, 1.58; H^δ 3.12, 3.46
Leu23		5.38	4.50	1.11, 1.37	H^γ 1.60; $C^\delta H_3$ 0.82, 0.86
Pro24			4.40	1.90, 2.27	H^γ 1.98, 2.03; H^δ 3.44, 3.74
Gln25	127.24	8.61	3.56	1.95, 2.10	H^γ 2.26, 2.30; N^ε 113.75
Val26	115.84	7.73	4.09	2.27	$C^\gamma H_3$ 0.96, 1.01
Leu27	122.37	7.37	4.42	1.67, 1.74	H^γ 1.74; $C^\delta H_3$ 0.91, 0.94
Leu28	123.72	8.03	4.82	1.41, 2.06	H^γ 1.78; $C^\delta H_3$ 0.41, 0.65
Ser29	116.49	9.16	4.78	3.58, 3.72	
Ser30	114.61	7.87	5.14	3.87, 4.06	
Trp31	120.64	8.37	5.89	2.93, 2.59	$H^{\delta1}$ 6.83; $H^{\varepsilon1}$ 9.60; $H^{\zeta2}$ 7.43; $H^{\eta2}$ 7.07; $H^{\varepsilon3}$ 6.83; $H^{\zeta3}$ 6.70; $N^{\varepsilon1}$ 134.71
Tyr32	117.65	8.90	4.58	2.89, 3.03	H^δ 7.01; H^ε 6.58
Pro33			5.10	2.42, 2.27	H^γ 2.19; H^δ 3.50, 3.66
Thr34	112.58	7.77	4.50	4.90	C^γH3 1.22
Ser35	118.61	8.69	4.36	3.96, 4.12	
Gln36	130.18	9.01	4.25	2.10, 2.19	H^γ 2.45, 2.49; N^ε 113.75
Leu37	121.89	8.19	4.26	1.58	H^γ 1.58; $C^\delta H_3$ 0.83, 0.89
Cys38	121.84	7.35	4.60	3.43, 2.73	
Ser39	122.08	8.61	4.15	3.91	
Lys40	123.92	8.05	4.74	1.68, 1.68	H^γ 1.29, 1.32; H^δ 1.44; H^ε 2.82; HN^η 7.63
Pro41			4.58	1.88, 2.26	H^γ 2.04; H^δ 3.60, 3.74
Gly42	113.12	8.34	4.16, 4.59		
Val43	123.29	8.68	4.64	1.62	C^γH3 0.34, 0.45
Ile44	127.82	8.83	4.55	1.74	H^γ 1.52, 1.89; $C^\gamma H_3$ 0.76; $C^\delta H_3$ 0.62
Phe45	126.47	9.11	5.23	2.98, 2.77	H^δ 7.08; H^ε 6.68; H^ζ 6.83
Leu46	126.95	8.94	5.38	1.68, 1.72	H^γ 1.70; $C^\delta H_3$ 0.60, 0.92
Thr47	118.52	9.35	5.00	4.88	$C^\gamma H_3$ 1.21; $O^{\gamma1}$H 6.21
Lys48	125.22	8.74	4.14	1.92, 1.72	H^γ 1.23, 1.33; H^δ 1.72; H^ε 3.00; HN^η 7.45
Arg49	118.57	7.49	4.50	2.15, 1.64	H^γ 1.75; H^δ 3.22; HN^ε 7.18
Gly50	111.96	7.98	3.66, 4.23		
Arg51	123.48	7.51	4.54	1.73, 1.89	H^γ 1.50; H^δ 3.14; HN^ε 7.19
Gln52	124.59	8.49	5.25	2.03, 1.95	H^γ 2.21, 2.47; N^ε 115.72
Val53	127.82	9.40	4.44	2.12	$C^\gamma H_3$ 0.87, 1.05
Cys54	129.94	8.85	5.32	3.29, 3.42	
Ala55	129.85	9.70	4.87	1.27	
Asp56	123.48	8.23	3.93	2.38, 1.37	
Lys57	127.68	7.69	3.69	1.40, 1.68	H^γ 1.12; H^δ 1.47; H^ε 2.82; HN^η 7.39
Ser58	116.83	8.20	4.15	3.84, 3.74	
Lys59	124.83	7.23	4.31	1.48	H^γ 1.24; H^δ 1.73; H^ε 2.94, 3.10
Asp60	128.16	9.07	4.15	2.84, 2.89	
Trp61	121.12	8.47	4.30	3.23, 3.48	$H^{\delta1}$ 7.67; $H^{\varepsilon1}$ 10.57; $H^{\zeta2}$ 7.26; $H^{\eta2}$ 6.70; $H^{\varepsilon3}$ 7.32; $H^{\zeta3}$ 6.50; $N^{\varepsilon1}$ 134.52
Val62	128.26	5.99	2.95	1.73	$C^\gamma H_3$ −0.79, 0.38
Lys63	123.34	7.56	4.03	1.73, 1.42	H^γ 1.24; H^δ 1.56; H^ε 2.82
Lys64	120.88	7.72	3.99	1.80	H^γ 1.41; H^δ 1.64; H^ε 2.96
Leu65	122.95	7.08	4.06	1.17, 2.03	H^γ 2.03; C^δH3 0.65, 0.84
Met66	120.69	7.93	2.92	1.80	H^γ 2.00
Gln67	117.17	7.10	4.27	2.22	H^γ 2.42, 2.55; N^ε 114.85
Gln68	120.16	7.50	4.37	2.23, 1.99	H^γ 2.39, 2.52; N^ε 114.66

Table 1 (*Continued*).
Chemical shifts of vMIP-II in H_2O solution at 308 K and pH 3.12

Residue	^{15}N	H^N	H^α	H^β	Others
Leu69	124.59	7.95	4.93	2.13, 1.54	H^γ 1.80; $C^\delta H_3$ 0.22, 0.97
Pro70			4.62	1.95, 2.28	H^γ 2.16; H^δ 3.88, 4.01
Val71	122.52	7.69	3.95	1.48	$C^\gamma H_3$ 0.58, 0.25
Thr72	127.77	8.58	3.98	3.67	$C^\gamma H_3$ 1.05
Ala73	132.11	8.11	4.22	1.27	
Arg74	127.34	7.82	4.02	1.52, 1.68	H^γ 1.38; H^δ 2.95; HN^ε 7.01

CC chemokines MIP-1β, RANTES, and MCP-1 is formed by a completely different set of residues located predominantly at the extended loop of the amino terminus and gives rise to an elongated, cylindrical molecule.

The different quaternary structure of CXC and CC chemokines offered an attractive rationalization for the receptor binding specificities of chemokines. Prior to the identification of vMIP-II, CXC chemokines could compete only with each other for binding to CXC chemokine receptors, while CC chemokines could only compete for binding to CC chemokine receptors [3]. This absolute specificity for binding and activation of chemokine receptors could be explained by invoking the recognition of the quaternary structures of chemokines by chemokine receptors. However, the physiological role of chemokine oligomerization and its relationship to receptor binding and activation is still unclear.

Studies of IL-8 have shown that IL-8 dimerizes in solution with a K_{dd} (dimer dissociation constant) of about 10–20 μM under conditions approaching physiological [23,24]. Because IL-8 binds its known receptors with nanomolar affinities ($K_d \sim 1$–2 nM for neutrophil receptors), and neutrophil chemotaxis and degranulation are induced over the same range, it was suggested that the monomeric form was the active species. A monomeric variant of IL-8 was produced by synthetic means [25] that effectively disrupted IL-8 dimer formation by altering the backbone hydrogen bond network at the dimer interface by incorporating *N*-methyl-Leu (instead of leucine) at position 25. This synthetic mutant was active in binding and activating neutrophils in vitro, providing evidence that the monomeric form of IL-8 is active.

More recent studies, however, provide evidence that dimerization may be important for biological activity. For example, it has been shown that IL-8 dimer formation may occur at concentrations that are considerably lower than 10 μM [26]. Studies with single-chain dimers of IL-8 have shown that dissociation of the dimeric species is not required for biological activity [27]. It is important to note that the oligomerization state of chemokines in vivo is not known. The presence of proteoglycans on the cell surface and in the extracellular matrix may influence the oligomerization state of chemokines and regulate their biological activity [28].

Our NMR data have allowed us to establish the oligomer state of the vMIP-II protein in solution. The absence of slowly exchanging amide protons for the N-terminal residues of vMIP-II suggests that the N-terminal region is not involved in inter-subunit interactions. In addition, no NOE contacts analogous to those that are found in chemokine dimers of either CC or CXC class were detected. The monomeric structure of vMIP-II was confirmed by employing pulsed field gradient NMR self-diffusion measurements using the water-suppressed LED pulse sequence [20]. The fits of the data to Eq. 1 (Section 2) are shown in Fig. 6. Using this method, the experimental measurements of the coefficient of self-diffusion, D_s, were $1.50 \pm 0.06 \times 10^{-6}$ cm^2/s and $1.09 \pm 0.05 \times 10^{-6}$ cm^2/s for vMIP-II and MIP-2, respectively. The D_s value of vMIP-II is in good agreement with the D_s value of 1.49×10^{-6} cm^2/s previously found for ubiquitin, a known monomeric protein that is similar in size (76 amino acid residues, 8.7 kDa) to vMIP-II [20]. The diffusion coefficient for vMIP-II at pH 7.0 is $1.52 \pm 0.04 \times 10^{-6}$ cm^2/s (data not shown), which is in good agreement with the data measured at pH 3.2. On the other hand, the D_s value of MIP-2, which has been recently shown to be a dimer in solution [29], is similar to the D_s value of 1.08×10^{-6} cm^2/s previously found for MCP-1, another

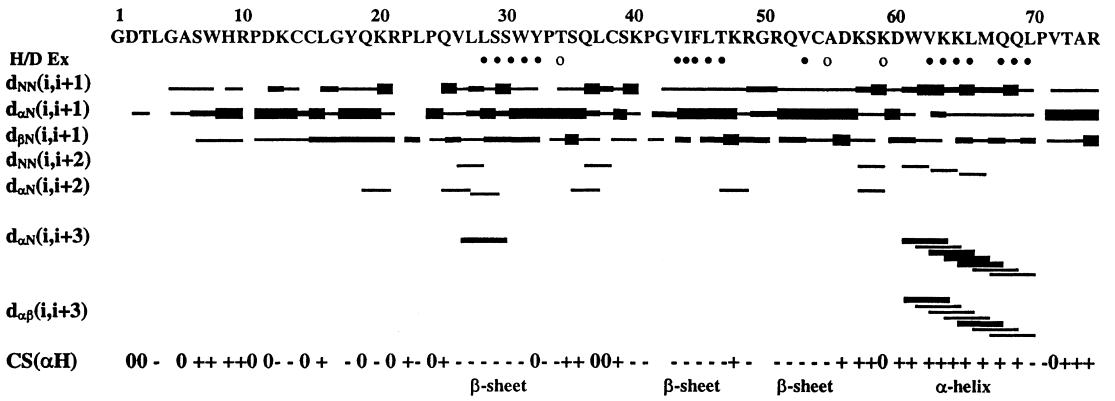

Fig. 5. Summary of the sequential NOE connectivities, backbone amide proton exchange rates, and chemical shift index of $C^\alpha H$ protons for vMIP-II. The relative strengths of the NOEs are indicated by the thickness of the lines. Slowly exchanging amide protons are indicated by a solid circle. More rapidly exchanging amide protons are indicated by an open circle. The chemical shift index of each $C^\alpha H$ is indicated by '−', '0', or '+', corresponding to the indices −1, 0, +1, respectively, described by Wishart et al. [21].

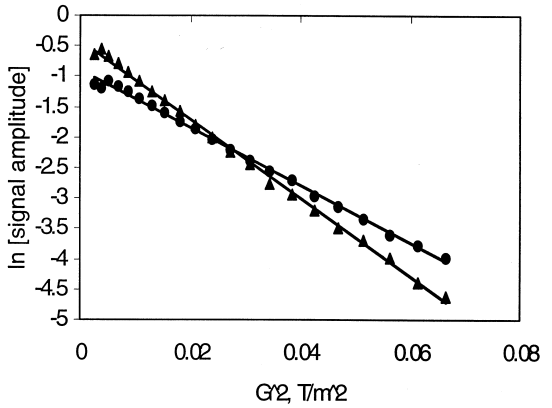

Fig. 6. Determination of the coefficients of self-diffusion, D_s, for MIP-2 and vMIP-II. Circles: MIP-2. Triangles: vMIP-II.

dimeric chemokine [20]. We therefore conclude that vMIP-II is a monomer in solution at NMR concentrations.

In summary, we have produced [SeMet]-vMIP-II by total chemical synthesis. The crystallization of this protein and determination of its selenium sites by Patterson methods indicate that chemical synthesis is a viable method for producing proteins for crystallographic studies. Solution studies of [SeMet]-vMIP-II indicate that the protein is a monomer in solution and has an α/β structure similar to other chemokines. These studies demonstrate that total chemical synthesis of proteins can be used to bypass the requirement for cloning, expression, and purification, and can accelerate functional and structural studies of newly identified small, soluble proteins or domains.

Acknowledgements: The authors wish to thank Dr. Xin Jia (The Burnham Institute, La Jolla, CA, USA) for providing us with the pulse sequence and macros for the self-diffusion measurements, and Paul Pepin for X-ray technical support. This work was supported in part by a research grant from the Arthritis Foundation to E.L.

References

[1] Hendrickson, W.A. (1991) Science 254, 51–58.
[2] Dawson, P.E., Muir, T.W., Clark-Lewis, I. and Kent, S.B.H. (1994) Science 266, 776–779.
[3] Baggiolini, M., Dewald, B. and Moser, B. (1997) Annu. Rev. Immunol. 15, 675–705.
[4] Moore, P.S. and Chang, Y. (1995) New Engl. J. Med. 332, 1181–1185.
[5] Moore, P.S., Boshoff, C., Weiss, R.A. and Chang, Y. (1996) Science 274, 1739–1744.
[6] Boshoff, C. et al. (1997) Science 278, 290–294.
[7] Kledal, T.N. et al. (1997) Science 277, 1656–1659.
[8] Otwinowski, Z. and Minor, W. (1997) Methods Enzymol. 276, 307–325.
[9] Braunschweiler, L., Bodenhausen, G. and Ernst, R.R. (1983) Mol. Physiol. 48, 535–560.
[10] Bax, A. and Davis, D.G. (1985) J. Magn. Reson. 65, 355–360.
[11] Griesinger, C., Otting, G., Wuthrich, K. and Ernst, R.R. (1988) J. Am. Chem. Soc. 110, 7870–7873.
[12] Kumar, A., Ernst, R.R. and Wuthrich, K. (1980) Biochem. Biophys. Res. Commun. 95, 1–6.
[13] Bodenhausen, G., Kogler, H. and Ernst, R.R. (1984) J. Magn. Reson. 58, 370–388.
[14] Bothner-By, A.A., Stephens, R.L., Lee, J.T., Warren, C.D. and Teanloz, R.W. (1984) J. Am. Chem. Soc. 106, 811–813.
[15] Rance, M., Sorensen, O.W., Bodenhausen, G., Wagner, G., Ernst, R.R. and Wuthrich, K. (1983) Biochem. Biophys. Res. Commun. 117, 479–485.
[16] States, D.J., Haberkorn, R.A. and Ruben, D.J. (1982) J. Magn. Reson. 48, 286–292.
[17] Smallcombe, S.H., Patt, S.L. and Keifer, P.A. (1995) J. Magn. Reson. A117, 295–303.
[18] McCoy, M.A. and Mueller, L. (1992) J. Am. Chem. Soc. 114, 2108–2110.
[19] Bodenhausen, G. and Ruben, D.L. (1980) Chem. Phys. Lett. 69, 185–188.
[20] Altieri, A.S., Hinton, D.P. and Bird, R.A. (1995) J. Am. Chem. Soc. 117, 7566–7567.
[21] Wishart, D.S., Sykes, B.D. and Richards, F.M. (1992) Biochemistry 31, 1647–1651.
[22] Fairbrother, W.J. and Skelton, N.J. (1996) in: Chemoattractant Ligands and Their Receptors (Horuk, R., Ed.) CRC Press, New York, NY.
[23] Burrows, S. et al. (1994) Biochemistry 33, 12741–12745.
[24] Paolini, J.F., Willard, D., Consler, T., Luther, M. and Krangel, M.S. (1994) J. Immunol. 153, 2704–2717.
[25] Rajarathnam, K., Sykes, B.D., Kay, C.M., Dewald, B., Geiser, T., Baggiolini, M. and Clark-Lewis, I. (1994) Science 264, 90–92.
[26] Lowman, H.B., Fairbrother, W.J., Slagle, P.H., Kabakoff, R., Liu, J., Shire, S. and Hebert, C.A. (1997) Protein Sci. 6, 598–608.
[27] Leong, S.R., Lowman, H.B., Liu, J., Shire, S., Deforge, L.E., Gillece-Castro, B.L., McDowell, R. and Hebert, C.A. (1997) Protein Sci. 6, 609–617.
[28] Hoogewer, A.J., Kuschert, G.S.V., Proudfoot, A.E.I., Borlat, F., Clark-Lewis, I., Power, C.A. and Wells, T.N.C. (1997) Biochemistry 36, 13570–13578.
[29] Shao, W., Jerva, L.F., West, J., Lolis, E. and Schweitzer, B.I. (1998) Biochemistry 37, 8303–8313.
[30] Wuthrich, K. (1986) NMR of Proteins and Nucleic Acids, Wiley, New York, NY.